Submitted to ADVANCED MATERIALS

Supporting Information

For *Adv. Mater.*, DOI: 10.1002/adma.201303520

Title: Tunable Delivery of siRNA from a Biodegradable Scaffold to Promote Angiogenesis *In Vivo*

Christopher E. Nelson[1], Arnold J. Kim[1], Elizabeth J. Adolph[2], Mukesh K. Gupta[1], Fang Yu[3], Kyle M. Hocking[1], Jeffrey M. Davidson[3], Scott A. Guelcher[2], Craig L. Duvall[1]*.

Supplemental Information

siRNA and primer sequences

Nucleic Acids were purchased from Integrated DNA Technologies (IDT, Coralville, IA, USA) based on the design principle that dsRNAs that contain a 27-mer antisense strand and a 25-mer sense strand have up to a 10-fold increased potency compared to 21-mer siRNA counterparts.[1] In addition, 2'-O-methyl (2-OMe) nucleotides were incorporated to improve duplex stability and nuclease resistance without affecting silencing activity or producing toxicity.[2] Minimal 2-OMe modifications on the backbone of the dsRNA were made to eliminate toll-like receptor activation and an immune response, with negligible effects on the potency of gene silencing.[3, 4] All listed siRNAs were screened *in vitro* before use *in vivo* (**Supplemental Table 1**). Fluorescent labels were used in portions of the manuscript including 6-FAM and cy5. These labels were obtained from IDT which are purified by HPLC.

Supplementary Table S1 – Nucleic acid sequences

Name	Sequence	mRNA Target Location	Silencing (in vitro 50nM)	Citation
dsDNA	S: 5′-FAM-GTCAGAAATAGAAACTGGTCATC-3′ AS: 5′-GATGACCAGTTTCTATTTCTGAC-3′	N/A	N/A	[5]
PPIB#1 NM_011149	S: 5′-GCCUUAGCUACAGGAGAGAAAGG[dA][dT]-3′ AS: 5′-AUCCUUUCUCUCCUGUAGCUAAGGCUA-3′	329	10%	N/A
PPIB#2 NM_011149	S: 5′-GCAUGGAUGUGGUACGGAAGGUG[dG][dA]-3′ AS: 5′-UCCACCUUCCGUACCACAUCCAUGCCC-3′	621	95%	N/A
PPIB#3 NM_011149	S: 5′-CGAUAAGAAGAAGGGACCUAAAG[dT][dC]-3′ AS: 5′-GACUUUAGGUCCCUUCUUCUUAUCGUU-3′	199	30%	N/A
Anti-Luciferase pGL2	S: 5′-CGUACGCGGAAUACUUCGAAAUG[dT][dC]-3′ AS: 5′-GACAUUUCGAAGUAUUCCGCGUACGUG-3′	230	55%	[6, 7]
Scrambled	DS Scrambled Neg – from IDT	N/A	N/A	
PHD2 #1	S: 5′-ACAUAGUUACAAGAGGAAACAAGCC – 3′ AS: 5′-GGCUUGUUUCCUCUUGUAACUAUGUUG – 3′	2094	78%	
PHD2 #2	S: 5′-ACCUAACAGUAGAUGGUUGCCACTG – 3′ AS: 5′-CAGUGGCAACCAUCUACUGUUAGGUCG – 3′	2053	67%	
PHD2 #3	S: 5′ – GGUACGCAAUAACUGUUUGGUAUTT -3′ AS: 5′-AAAUACCAAACAGUUAUUGCGUACCUU – 3′	1278	8.2%	
PPIB Primers	FWD: 5′-TTCCATCGTGTCATCAAG-3′ REV: 5′-GAAGAACTGTGAGCCATT-3′			
GAPDH Primers	FWD: 5′-CTCACTCAAGATTGTCAGCAATG-3′ REV: 5′-GAGGGAGATGCTCAGTGTTGG-3′			
STAT-1 Primers	FWD: 5′-GCAACTGGCATATAACTT-3′ REV: 5′-GTGACATCCTTGAGATTC-3′			
TNFα Primers	FWD: 5′-CAAAGGGATGAGAAGTTC-3′ REV: 5′-TGAGAAGATGATCTGAGT-3′			
PHD2 Primers	FWD: 5′-ATCTAACAGGTGAGAAAGGT-3′ REV: 5′-ACAGAAGGCAACTGAGAG-3′			
VEGF Primers	FWD: 5'-CCTGGTGGACATCTTCCAGGAGTA-3' REV: 5'-CTCACCGCCTTGGCTTGTCACA-3'			
FGF-2 Primers	FWD: 5'-CTCCAGTTGGTATGTGGCACT-3' REV: 5'-CAGTATGGCCTTCTGTCCAGG-3'			

Poly[DMAEMA$_{71}$-b-(BMA$_{103}$-co-PAA$_{68}$-co-DMAEMA$_{57}$)]and nanoparticle (NP) characterization

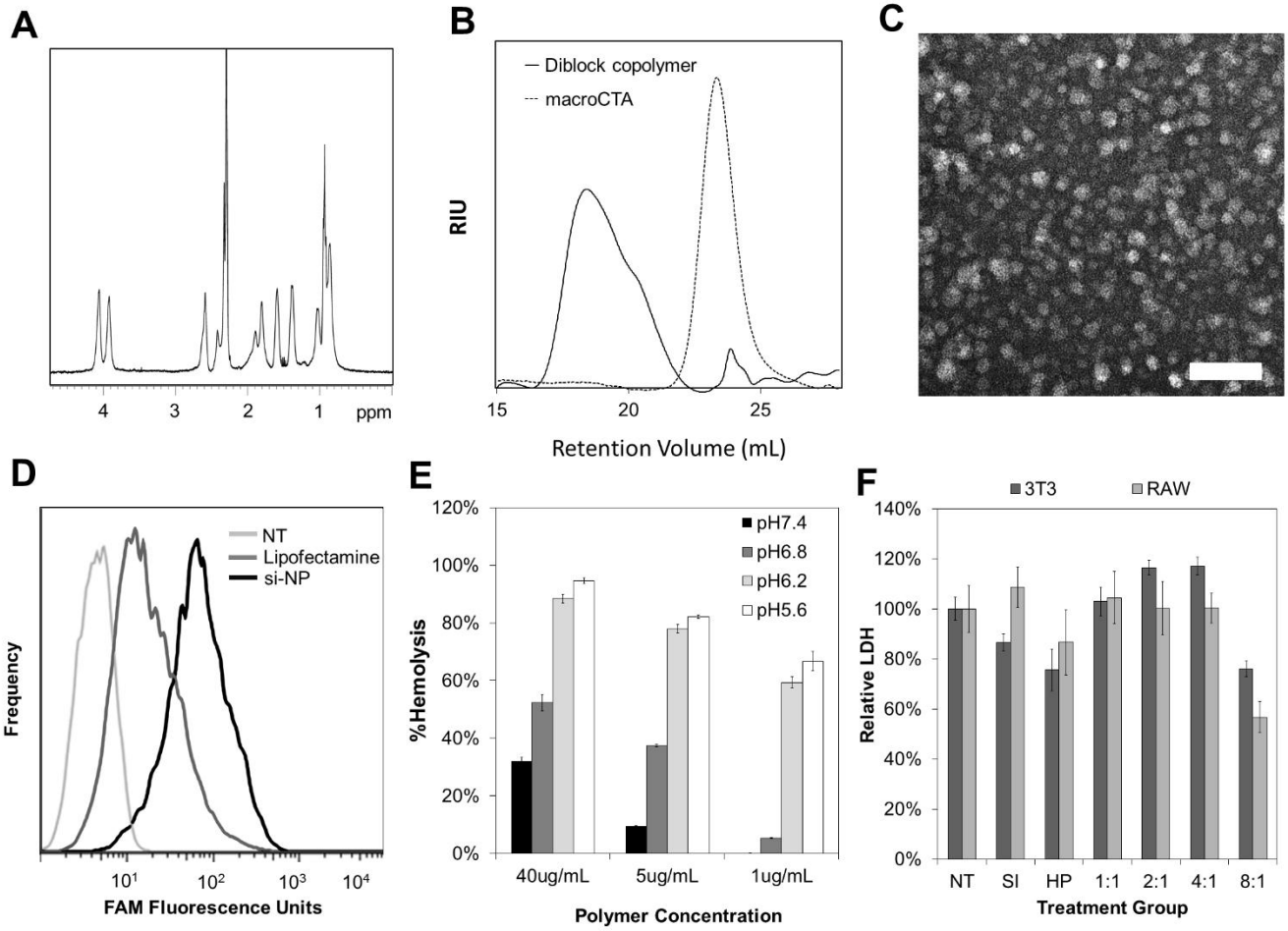

Supplementary Figure S1: Characterization of Poly[DMAEMA$_{71}$-b-(BMA$_{103}$-co-PAA$_{68}$-co-DMAEMA$_{57}$)] and self-assembled nanoparticles. These data are representative of the polymer and the NPs used in this study. The formulations are similar to those characterized in previous publications.[8-10] **A**) H^1 NMR of the polymer was used to determine percent composition of each monomer. **B)** GPC for the DMAEMA macroCTA and the diblock copolymer were utilized to determine molecular weight and polydispersity. **C)** TEM of the NPs after micellar assembly of poly[DMAEMA$_{71}$-b-(BMA$_{103}$-co-PAA$_{68}$-co-DMAEMA$_{57}$)] shows a uniform structure of the particles(Scale = 100 nm). **D)** Flow cytometry of NIH3T3 mouse fibroblast uptake of fluorescently labeled dsDNA loaded into si-NPs and Lipofectamine 2000 relative to control cells with no treatment demonstrate a higher level of uptake for NPs. **E)** The hemolysis assay was used to demonstrate that the pH-dependent membrane disruptive activity of the NPs is appropriately tuned for endosomlytic behavior. **F)** All NP formulations used in this study were cytocompatible in NIH3T3 fibroblasts (3T3s) and RAW 264.7 macrophages (RAW) compared to a no treatment (NT) control, siRNA only (SI), and HiPerFect (HP) as shown by this LDH assay (note that 4:1 charge ratio (NH_3+/PO_4-) was utilized for all si-NPs formulations in these studies).

The Weibull model for release kinetics

Equation S1: $$\frac{M_t}{M_\infty} = 1 - exp(-a \cdot t^b)$$

The Weibull model describes the % of mass of si-NPs released (M_t/M_∞) at time t, where *a* is a constant based on the system, and *b* is a constant based on the release kinetics. Previous reports suggest that values of b < 0.75 indicate that Fickian diffusion is the dominant release mechanism.[11, 12]

Supplementary Table S2. Weibull Model Analysis – In Vitro Release Data

Formulation	a	b	R^2
LTI – 0T	0.0273	0.5511	0.992
LTI – 1.25T	0.1582	0.3488	0.9183
LTI – 2.5T	0.4797	0.3648	0.869
LTI – 5T	1.729	0.4448	0.8736
HDIT – 0T	0.026	0.336	0.9792
HDIT – 1.25T	0.0399	0.3828	0.9764
HDIT – 2.5T	0.0691	0.4818	0.9689
HDIT – 5T	0.1451	0.4402	0.99

Supplementary Table S3. Weibull Model Analysis – In Vivo Release Data

Formulation	a	b	R^2
LTI – 0T	0.433	0.3052	0.8912
LTI – 1.25T	0.9976	0.1599	0.8236
LTI – 5T	1.336	0.2436	0.7426
HDIT – 0T	0.2912	0.3707	0.8921
HDIT – 1.25T	0.4716	0.3591	0.9295
HDIT – 5T	0.867	0.317	0.8564

Representative release kinetics images

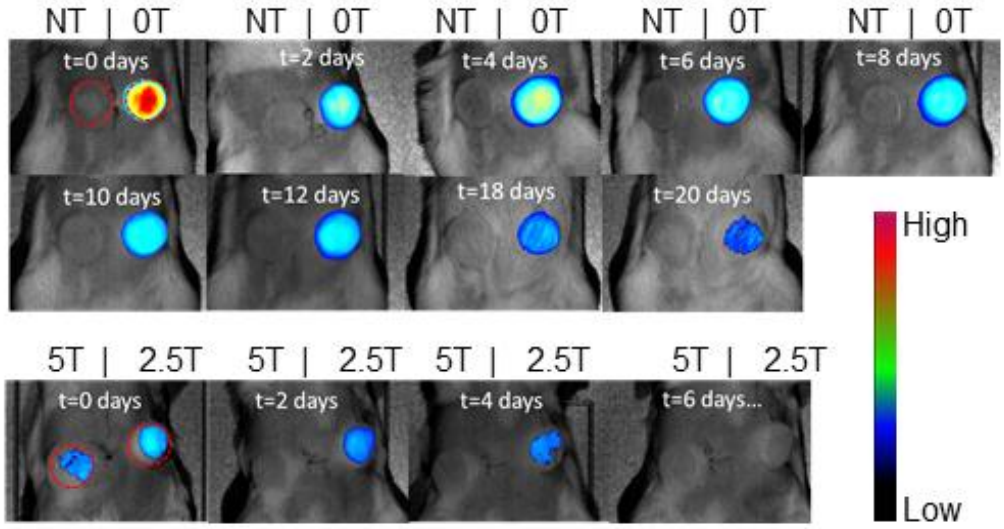

Supplementary Figure S2. Visual Representation of Release Kinetics. The release kinetics data (Figure 2K, 2L) was calculated by loading the si-NPs with Cy5-labeled siRNA and measuring the change in fluorescence within the PEUR scaffolds with intravital imaging. In each case, a region of interest (shown in red) was defined that contained just the scaffold, and the average fluorescence was calculated and compared to the initial image of PUR before implantation (after compensating for loss of fluorescence from imaging through the tissue). The representative images above visually demonstrate the rate of loss of Cy5 fluorescence within the scaffold.

The 4 parameter logistic model used for IC_{50} and dose response analysis

Equation 2: $$\%\text{Expression} = \frac{-1}{\left(1+\left(\frac{x}{IC_{50}}\right)^{b}\right)} + 1$$

Temporal control of the gene silencing profile for scaffolds composed of HDIT PEUR

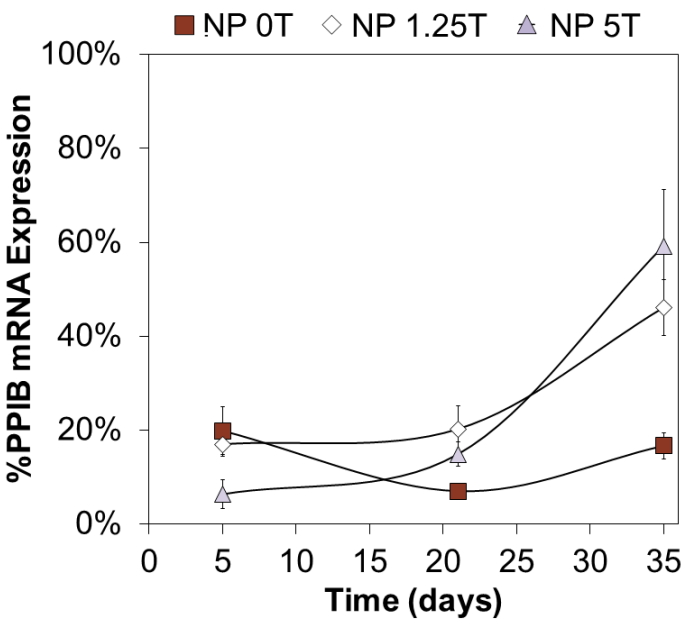

Supplementary Figure S3: PCR for PPIB expression in the HDIt scaffolds using the same method described for the LTI data shown in Figure 3C. The temporal gene silencing profile was similar to that seen with the LTI based scaffolds.

Infiltration of PUR scaffolds. Effect of formulation

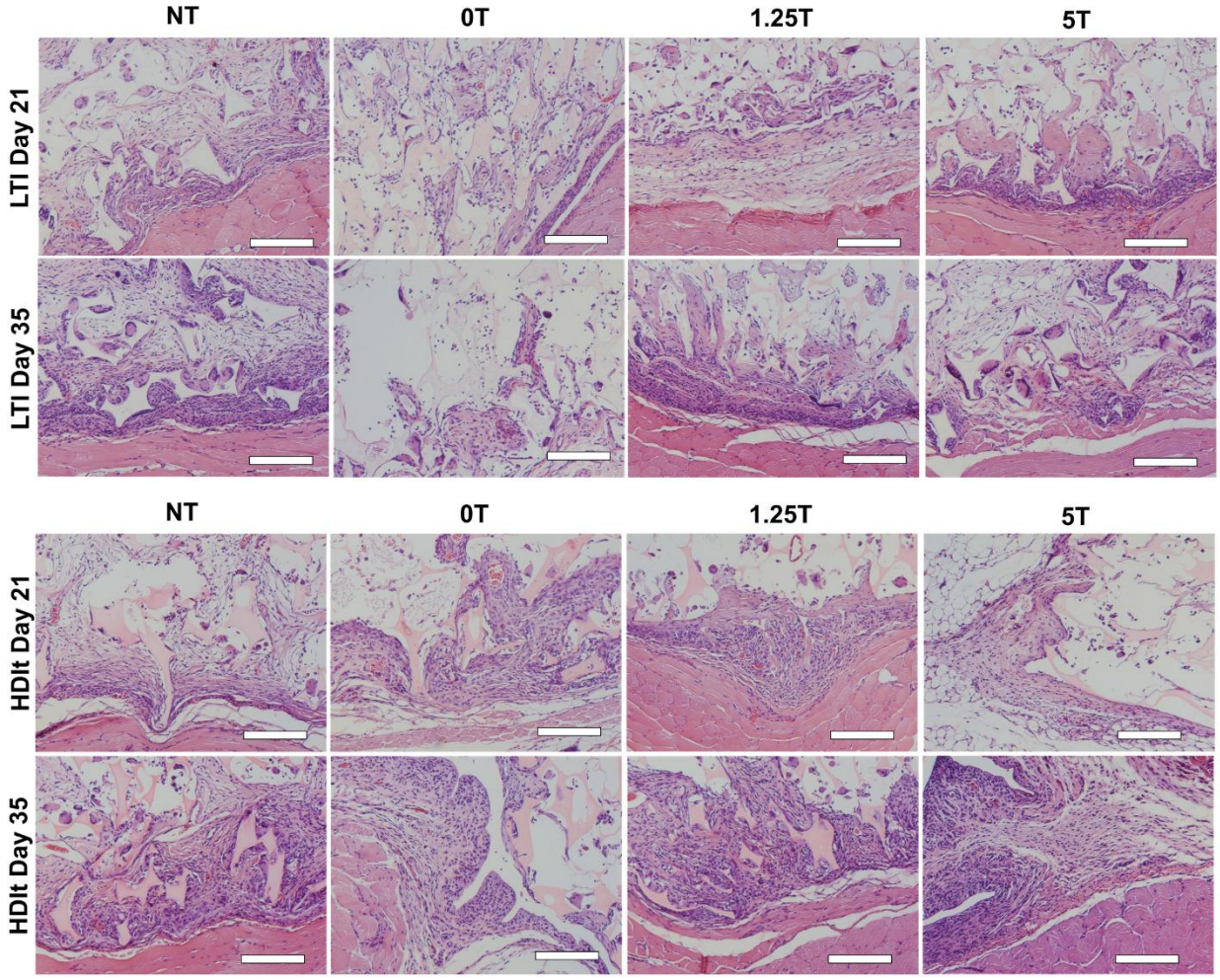

Supplementary Figure S4 - Microscopic view of Hematoxylin and eosin (H&E) stained sections shows the morphology and the degree of infiltration at day 21 and day 35 in LTI and HDIt based scaffolds demonstrating similar levels of cellular infiltration. Scale bar = 200 um. (n=1)

PCR for TNFα and STAT-1 markers of inflammation and TLR activation

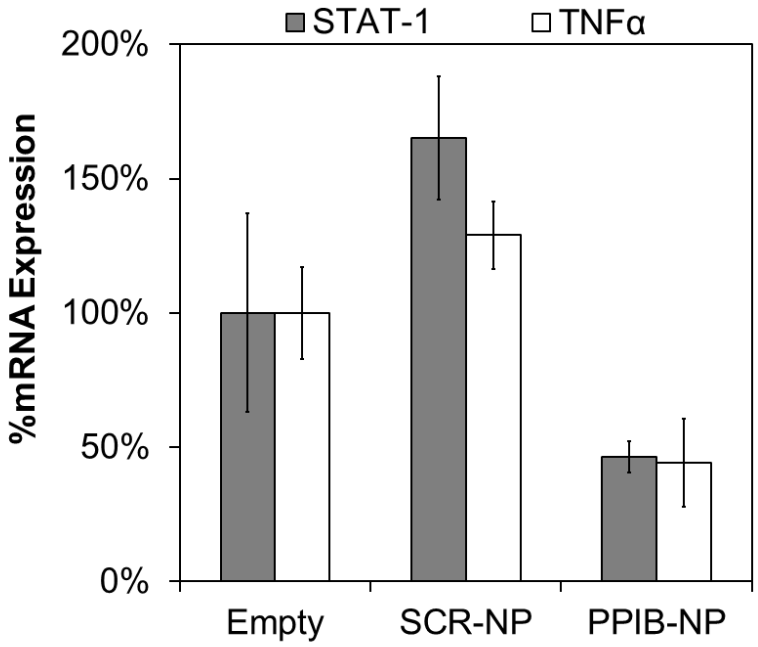

Supplementary Figure S5: PCR for STAT-1 and TNFα normalized to GAPDH expression indicates that the delivery platform does not activate nonspecific inflammation or TLRs. A statistically insignificant increase in the scaffolds loaded with si-NPs containing scrambled siRNA may indicate a small non-specific inflammatory response to either the scrambled siRNA or the polymer, but is not indicative of the orders of magnitude increase in STAT-1 produced by TLR activation.[13] In the scaffolds containing si-NPs loaded with PPIB siRNA (PPIB-NP), there was a significant decrease in both STAT-1 and TNFα, suggesting anti-inflammatory activity was produced by silencing the model gene PPIB. This aligns with the known functions of PPIB as a pro-inflammatory secretory product of macrophages[14] that is increased in response to inflammatory stimuli[15] and that plays a role in adhesion of T-lymphocytes.[16] It has also been previously identified that inhibition of CD147 and PPIB interactions is a viable therapeutic strategy for reduction in inflammation.[17] Although it is outside the scope of the current report, this result indicates that potent PPIB silencing has the potential to be used as an anti-inflammatory therapy.

Supplemental methods

1. NP characterization

The diblock copolymer used in this study is from the same synthesis previously reported.[10] The polymers were characterized by gel permeation chromatography (GPC, Shimadzu Corp., Kyoto, Japan) in DMF with 0.1 M LiBr using an inline Wyatt miniDAWN TREOS light scattering detector (Wyatt Technology Corp., Santa Barabara, CA) and H^1 NMR (Bruker 400 MHz Spectrometer equipped with a 9.4 T Oxford magnet) for molecular weight and composition. Transmission Electron Microscopy (TEM, Philips CM20 Transmission Electron Microscope, EO, Netherlands) was used to evaluate micelle diameter and morphology. A gel retardation assay was used to select the charge ratio (NH_3+/PO_4-), and 4:1 was used for all experiments. Flow cytometry was performed on NIH3T3 fibroblasts treated with a concentration of 50nM FAM labeled dsDNA (**Supplemental Table S1**) and measured with a BD FACSCalibur flow cytometer (San Jose, CA). The data was analyzed using FlowJo software (version 7.6.4 Ashland, OR). A pH-dependent hemolysis assay was performed using a standardized protocol[18] to characterize pH-dependent membrane disruption of the polymer at concentrations of 40 µg/mL, 5µg/mL, and 1µg/mL in buffers of pHs 7.4, 6.8, 6.2, and 5.8. The percent hemolysis was calculated using data collected using a plate reader (Infinite F500, Tecan Group Ltd., Mannedorf, Switzerland) to measure absorbance at 541 nm. Cellular toxicity was analyzed at a concentration of 50nM siRNA with varying charge ratios up to N:P of 8:1 using an LDH cytotoxicity kit (Roche, Basal, Switzerland).

2. Western blot

Frozen samples were extracted with UDC buffer (8 M urea, 10 mM dithiothreitol (DTT), 4% CHAPS containing Phosphatase I and II protease inhibitor cocktail (Sigma, St. Louis, MO)) by vortexing at room temperature overnight and centrifugation at 14,000 rpm for 15 min at 4°C. Soluble protein concentrations were determined using the Bradford assay (Pierce Chemical, Rockfort, IL). Equal amounts (30 µg) of proteins were added to Laemmli sample buffer (Bio-Rad laboratories, Inc. Hercules, CA), heated for 5 min at 100°C, and separated on 12% SDS polyacrylamide gels. Proteins from the gels were transferred onto nitrocellulose membranes (Li-COR Biosciences, Lincoln, NE) and blocked with blocking buffer for 1 hour at room temperature(Li-COR Biosciences, Lincoln, NE) prior to incubation overnight at 4°C with antisera against PPIB (1:2000,Sigma) and ß-actin (1:250,Santa Cruz Biotechnology). Membranes were washed three times with TBS containing Tween 20 (0.1%) (TBST) and incubated with 680 nm and 800 nm infrared-labeled secondary antibodies (Li-Cor, Lincoln, NE) for 1h at room temperature. The membranes were subsequently washed with TBST, and protein-antibody complexes were visualized and quantified using the Odyssey direct infrared fluorescence imaging system (Li-Cor Biosciences NE).

3. Cardiac Perfusion and microCT

Mice were sacrificed by CO_2 inhalation and perfused with normal PBS containing 4 mg/mL papaverine hydrochloride (Sigma) and 100 U/mL Heparin followed by 10% neutral buffered formalin, followed by PBS with papaverine hydrodhloride and Heparin. Next, 30 mL of the lead chromate based contrast agent Microfil® (Flowtec) was injected into the left ventricle and allowed to cure overnight at 4°C. Implants were retrieved and scanned using a microCT (uCT 50, Scanco Medical AG, Brüttisellen Switzerland) for vessel morphology, vascular volume and vascular thickness. Regions of Interest were selected by each slice selecting area inside the scaffold.

Supplemental references

[1] D. H. Kim, M. A. Behlke, S. D. Rose, M. S. Chang, S. Choi, J. J. Rossi, *Nat. Biotechnol.* **2005**, *23*, 222-226.
[2] M. A. Behlke, *Oligonucleotides* **2008**, *18*, 305-319.
[3] A. Judge, I. MacLachlan, *Hum. Gene Ther.* **2008**, *19*, 111-124.
[4] A. D. Judge, G. Bola, A. C. Lee, I. MacLachlan, *Mol. Ther.* **2006**, *13*, 494-505.
[5] N. P. Truong, Z. Jia, M. Burgess, L. Payne, N. A. McMillan, M. J. Monteiro, *Biomacromolecules* **2011**, *12*, 3540-3548.
[6] J. R. de Wet, K. V. Wood, M. DeLuca, D. R. Helinski, S. Subramani, *Mol. Cell. Biol.* **1987**, *7*, 725-737.
[7] S. M. Elbashir, J. Harborth, W. Lendeckel, A. Yalcin, K. Weber, T. Tuschl, *Nature* **2001**, *411*, 494-498.
[8] A. Convertine, D. Benoit, C. Duvall, A. Hoffman, P. Stayton, *J. Control. Release* **2009**, *133*, 221-229.
[9] A. J. Convertine, C. Diab, M. Prieve, A. Paschal, A. S. Hoffman, P. H. Johnson, P. S. Stayton, *Biomacromolecules* **2010**, *11*, 2904-2911.
[10] C. E. Nelson, M. K. Gupta, E. J. Adolph, J. M. Shannon, S. A. Guelcher, C. L. Duvall, *Biomaterials* **2012**, *33*, 1154-1161.
[11] B. Li, K. V. Brown, J. C. Wenke, S. A. Guelcher, *J. Control. Release* **2010**, *145*, 221-230.
[12] V. Papadopoulou, K. Kosmidis, M. Vlachou, P. Macheras, *Int. J. Pharm.* **2006**, *309*, 44-50.
[13] C. A. Sledz, M. Holko, M. J. de Veer, R. H. Silverman, B. R. G. Williams, *Nat. Cell. Biol.* **2003**, *5*, 834-839.
[14] B. Sherry, N. Yarlett, A. Strupp, A. Cerami, *P. Natl. Acad. Sci. USA* **1992**, *89*, 3511-3515.
[15] A. Melchior, A. Denys, A. Deligny, J. Mazurier, F. Allain, *Exp. Cell. Res.* **2008**, *314*, 616-628.
[16] F. Allain, C. Vanpouille, M. Carpentier, M.-C. Slomianny, S. Durieux, G. Spik, *P. Natl. Acad. Sci. USA* **2002**, *99*, 2714-2719.
[17] V. Yurchenko, S. Constant, E. Eisenmesser, M. Bukrinsky, *Clin. Exp. Immunol.* **2010**, *160*, 305-317.
[18] B. C. Evans, C. E. Nelson, S. S. Yu, K. R. Beavers, K. A. J., H. Li, H. M. Nelson, T. D. Giorgio, C. L. Duvall, *J. Vis. Exp.* **2012**, e50166.